

CONCEPT DEVELOPMENT OF INCLINOMETER FOR REAL-TIME DATA COLLECTION IN SLOPE MOVEMENT DETECTION

AINA SYAHIRAH AHMAD ISHAK¹, JESTIN JELANI^{1,*},
SYED MOHD FAIRUZ SYED MOHD DARDIN²,
ZUHAIRI ABDUL RASHID³, ZULIZIANA SUIF¹

¹Department of Civil Engineering, Faculty of Engineering, National Defence University of Malaysia, 57000, Kuala Lumpur, Malaysia

²Department of Electric and Electrical Engineering, Faculty of Engineering, National Defence University of Malaysia, 57000, Kuala Lumpur, Malaysia

³Malaysian Armed Forces, Malaysia

*Corresponding Author: jestin@upnm.edu.my

Abstract

Natural disasters such as landslides are unpredictable phenomena resulting in many casualties and economic losses around the world. Continuous monitoring of landslides is important to provide information of slope movement, stress state, and historical trend as a basis for early warning purposes. A variety of measurement methods of slope movement detection have been developed over the past few decades. However, a real-time continuous monitoring of slope movement at deeper ground is still insufficient and requires significant improvement. This paper presents the concept of a 3-dimensional real-time slope movement detection using a newly developed sensor, namely Multi-Point Fixed Inclinator (MPFI). The MPFI is a single module prototype MPU-9250 device developed and incorporated in the micro-electromechanical system (MEMS) which consists of 3-axes of gyroscope, 3-axes of accelerometer, and 3-axes of magnetometer. Calibration for magnetometer, gyroscope and accelerometer were conducted by considering all axes by averaging the static measurement of the sensor. In this paper, basic measuring principles for deep displacement monitoring are discussed and the concept development of MPFI is described based on the principle of real-time landslide monitoring. The use of MPFI sensor will have the capability to determine slope displacement and rate of movement parameters in three dimensions for landslide early warning system.

Keywords: Inclinator, Sensor calibration, Slope failure, Slope monitoring.

1. Introduction

Landslide is among the prominent geological hazards due to movement of rock mass, soil, or debris down a slope by gravity force [1]. It occurs when shear stress exceeds shear strength of soil and subsequently triggers a failure by slope movement. The movement is a complex process that depends on many factors and some external factors include rainfall, excessive surcharge load, groundwater fluctuation, geological conditions and others [2].

It is well known that landslide has a huge impact on human life and economic losses. Vega et al. [3] mentioned that 0.53% of deaths and 14% of economic losses exceeding \$1 billion reported worldwide are due to landslide. In Malaysia particularly, there were 28 major slope failures reported with an estimated loss of US \$1 billion from 1973-2007 and a total fatality of more than 100 lives [3-5]. Considering these impacts and complexities of landslide, an early warning system is of paramount necessity to reduce such losses [6, 7].

Over the past few decades, researchers have developed and adopted a variety of landslide early warning systems for monitoring and detecting slope movement at deeper ground. To meet the needs of modern monitoring purpose, the development has gradually reflected the following features, namely wireless sensing network, remote monitoring, automated, distributed and high precision devices, where this development has facilitated the transmission of real-time data from site to remote station [8, 9].

The existing instrument for measuring deep slope movement includes Acoustic Emission, Time Domain Reflectometry, Fiber Bragg Grating and inclinometer sensor. Acoustic Emission (AE) is used as one of the continuous real-time monitoring systems that can detect the risk of soil instability. The soil structure undergoing deformation will generate AE from inter-particle friction that can be measured using alarms of acoustic sensor encased in steel tubes in the ground [10].

The Time Domain Reflectometry (TDR) is a measurement technique using coaxial cable and cable testers buried in the ground for coupling the deformation of the slope. The deformation is detected using reflection wave impedance analysis. TDR detects the amount of deformation and presents the increased value of the reflection coefficient with increasing deformation [9, 11].

The Fiber Bragg Grating (FBG) on the other hand, is a fiber optic sensing technique to measure the strain or temperature of different structures. FBG is a sensor consisting of a band of material with different refractive indices, which serves to block rays of certain wavelengths. Only the central light wavelength corresponding to the local modulation period can be reflected. Either strain or temperature will change the Bragg wavelength through the expansion or the contraction of the grating periodicity [9, 12].

The conventional inclinometers consist of one or two tilt sensors capable of measuring the tilt and lateral displacement of subsurface soil or rock. Inclinometers can be installed in a borehole up to 200m deep where the depth of the borehole depends on the depth of failure slope. Typically, inclinometers are based on relatively stable soil layers to determine the displacement [9, 13].

This paper describes a newly developed MPFI sensor to improve the performance of conventional inclinometers, which unable to provide 3D profile of

deep slope movement measurement. Calibration and correction of measurement data, installation methods and laboratory experiments are described in this paper. The output of this research will be used for a real-time slope monitoring system.

2. Methods

In this study, the proposed inclinometer sensor consists of MEMS sensor which is the MPU-9250 that normally used in motion tracking device as shown in Fig. 1. The MPU-6500 houses 3 different sensors in a form of three-axis gyroscope, accelerometer and three-axis magnetometer.



Fig. 1. MPU-9250 sensor module.

The sensors can act as an Initial Measurement Unit (IMU) by combining all 9-axes motion tracking with an on-board Digital Motion Processor (DMP). The communication of this sensor is performed using I2C which directly provides a complete 9-axis Motion Fusion.

2.1. The proposed inclinometer design and operation

The combination of gyroscope, accelerometer, and magnetometer in this IMU aims to continuously calculate and collect data in terms of rotation, speed, and position of slope movement. In general, the purpose of the proposed inclinometer is to collect real-time data information in the form of angles and transfer the data to communication nodes. Data determined by its roll (ρ), pitch (θ), and yaw (θ) angles are taken using IMU sensor readings at each instant of time.

To set up the hardware, the sensor device is connected to an Arduino Nano microcontroller board using the I2C communication interface. This board is used as the interface to continuously read the data from the MPU-9250 sensor. Figure 2 and 3 show the conceptual and prototype models of the proposed MPFI sensor respectively.

The sensor uses an Analog-to-Digital Converter (ADC) to convert the obtained data to digital values. Data packets are then created from digital values obtained from the ADC to be used for communication protocol via the I2C. The Arduino Nano microcontroller board is used as part of system development for reading and processing data before being transmitted to the server.

The proposed experimental test setup for small-scale slope model with MPFI sensor is shown in Fig. 4. There are five sensors placed in the slope model and

arranged vertically in two separated boreholes. Three and two MPFI sensors are installed at the crest and toe of the slope respectively to detect slope movement.

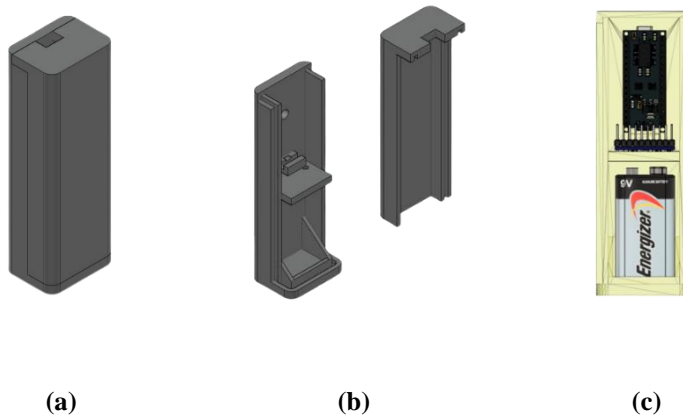


Fig. 2. Conceptual model of MPFI sensor (a) Outer shell of MPFI (b) Inner casing of MPFI (c) The component of MPFI..



Fig. 3. Prototype model of MPFI sensor.

Figure 5 shows the laboratory setup for the silica sand slope model placed in an acrylic box with dimensions of 1.5m x 0.5m x 1.0m. The slope model is subjected to a surcharge load up to 10kPa to initiate a landslide.

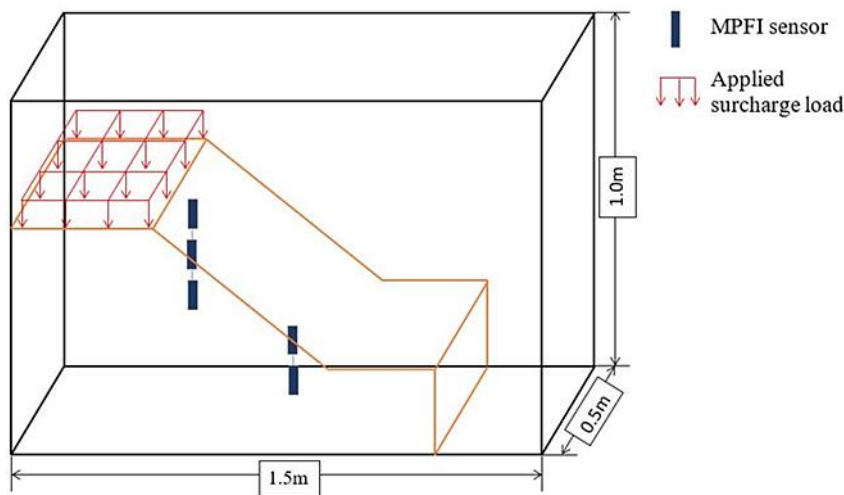


Fig. 4 The arrangement of MPFI sensor.

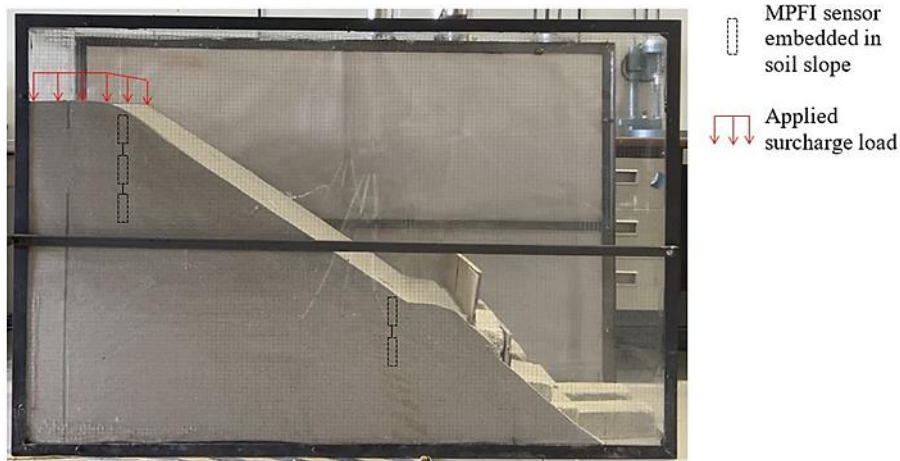


Fig. 5. The laboratory experimental setup.

2.2. Sensor fusion of MPU-9250

The gyroscope used in this study measures the rate of change of an orientation angle to determine the angular velocity of a slope. Measurement of gyroscope angles are calculated by initializing the sensor with a known value. The angular velocity (ω) is measured for three different axes (x, y and z) at predetermined time intervals (Δt). The value of angular velocity (ω) is multiplied by the time interval (Δt) to obtain the change in position of the angle, where the value of the new orientation angle can be obtained by adding the original angle with the computed change at each time.

However, reading gyroscope data using integration will result in many additions of small calculation intervals. Therefore, small systematic errors will be produced and magnified over time, or what is called the gyroscopic drift. As a result, gyroscope data will become increasingly inaccurate over a long period of time due to the errors. This effect has resulted in a combination of gyroscope sensors with additional sensors, such as accelerometers and magnetometers to correct for this effect. The combination of sensors is often referred to as sensor fusion.

For accelerometer, the angles are determined by using the gravity vector and its projection on the accelerometer axes. There are three types of trigonometric function that are available for conversion from acceleration to angle, namely the inverse tangent function, the inverse sine function, and the inverse cosine function. Nevertheless, the inverse tangent function is used as it is more accurate, requires less computation than other algorithms, and has a constant effective incremental sensitivity [14, 15].

Figure 6 shows the angle of each axis of the accelerometer is determined separately from the reference position where ρ is the angle between the x-axis of accelerometer and the horizontal line, ϕ is the angle between the horizontal line and the y-axis, and θ is the angle between the z-axis and Earth's gravity vector, while A_x , A_y , and A_z are the components of gravity measured by each axis of accelerometer.

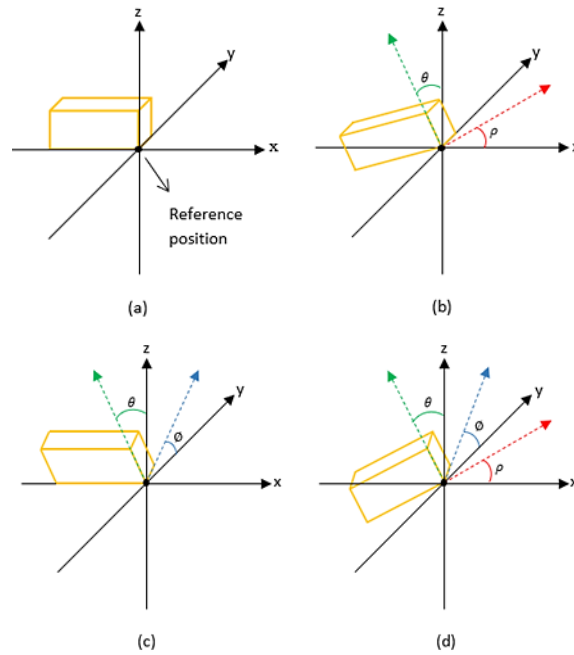


Fig. 6. The angles of each axis based on reference position. (a) The initial inclination angles based on reference position; (b) The illustration of the relationship between angles θ and ρ ; (c) The illustration of the relationship between angles θ and ϕ ; (d) Three inclination angles of the inclinometer.

Equations (1), (2) and (3) below show an inverse-tangent-based algorithm for conversion of accelerometers to angle.

$$\rho = \left(\frac{A_x}{\sqrt{A_y^2 + A_z^2}} \right) \quad (1)$$

$$\phi = \left(\frac{A_y}{\sqrt{A_x^2 + A_z^2}} \right) \quad (2)$$

$$\theta = \left(\frac{\sqrt{A_y^2 + A_x^2}}{A_z} \right) \quad (3)$$

where: A_x is component of gravity measured by x-axis of accelerometer, A_y is component of gravity measured by y-axis of accelerometer and A_z is component of gravity measured by z-axis of accelerometer. The angles are defined as: ρ = Roll angle, ϕ = Pitch angle, and θ = Yaw angle.

2.3. Sensor calibration

In applying sensing modules in slope monitoring, several challenges are often encountered in obtaining accurate measurements. Some of the factors affecting accuracy are bias and noise errors which can directly affect the quality of the collected data. To ensure accurate reading of the sensors, calibration is important

to minimize the error distribution of the sensing modules and provide a predictable output for the measured data.

The IMU has been calibrated at the factory for system errors. However, the sensing module will experience some errors during its use. For instance, the gyroscope reading is not fixed after each power-up which causes the reading to drift. This is commonly known as zero bias which affects the stability of the data, and the bias needs to be corrected before use. For accelerometer, some force is applied during vibration as it moves and rotates which causes the tendency for the data to fluctuate and degrade the data acquisition accuracy. To calibrate the errors of both gyroscope and accelerometer readings, static measurement data for the x, y and z axes need to be averaged and used as calibrated values for subsequent measurements [16, 17].

In addition, readings of magnetometer are easily affected if it experiences errors due to conditions called Hard-iron and Soft-iron errors which adversely affect the accuracy of yaw angle. Hard-iron errors are caused by metallic objects on the magnetometer circuit board that produce static magnetic field. This type of error results in an offset the center of the ellipsoid from the origin. Meanwhile, Soft-iron errors are caused by objects close to the sensor that distort the surrounding magnetic field. This type of errors does not produce an ideal measurement where it causes the magnetometer data to transform into an ellipsoid instead of a perfect sphere [18].

Therefore, calibration of magnetometer readings which involves the fitting of an offset ellipsoid into a sphere centered at the origin can be investigated via Matlab simulation. Here, sphere fitting algorithm is used in which offset ellipsoid data will be generated if these effects exist. To overcome and reduce errors, the values of Hard-iron and Soft-iron correction matrix obtained through Matlab analysis will be taken as calibration parameters to enter the new ellipsoid fitting process. The ellipsoid fitting process can calculate the correction values of Hard-iron and Soft-iron errors.

3. Results and Discussion

The basic function of the inclinometer was realized through software and hardware designs with the application of angle measurement principles of MPU-9250 module sensor. After parameters setup, raw data of each axis of gyroscope, accelerometer and magnetometer sensor are read through I2C protocol.

Since gyroscope data measurements are prone to significant drift over time, vibration will cause severe fluctuations in accelerometer data acquisition, and magnetometer is prone to Hard-iron errors and Soft-iron errors, so calibration is required to compensate for all errors and provide accurate results.

For gyroscope and accelerometer, calibration was performed by taking the mean values in the data measurements for three different axes as shown in Table 1. The calibrated values will be used as compensation values for subsequent measurements.

Table 1. Mean values of gyroscope and accelerometer for x, y, and z axes.

Axis	Gyroscope ($^{\circ}/s$)	Accelerometer (g)
x	0.68	-2.00
y	6.87	2.00
z	-0.56	-2.00

For magnetometer calibration, a set of data were collected from MPU-9250 sensor module and calibrated via MATLAB. The three-dimensional (3D) data figure of the uncalibrated and calibrated magnetometer data is shown in Figs. 7(a) and 7(b) respectively. Figure 7(a) represents the magnetometer measurement data sets form an offset ellipsoid data due to the existing Hard-iron and Soft-iron errors.

Equations (4) and (5) below are the correction matrix of Hard-iron and Soft-iron obtained from magnetometer calibration.

$$C_s = \begin{bmatrix} 0.9649 & 0.0416 & -0.0246 \\ 0.0416 & 0.9635 & -0.0335 \\ -0.0246 & -0.0335 & 1.0794 \end{bmatrix} \quad (4)$$

$$C_H = [-25.2573 \ 12.9978 \ -12.1779] \quad (5)$$

where: C_s is correction matrix for Soft-iron and C_H is correction matrix for Hard-iron.

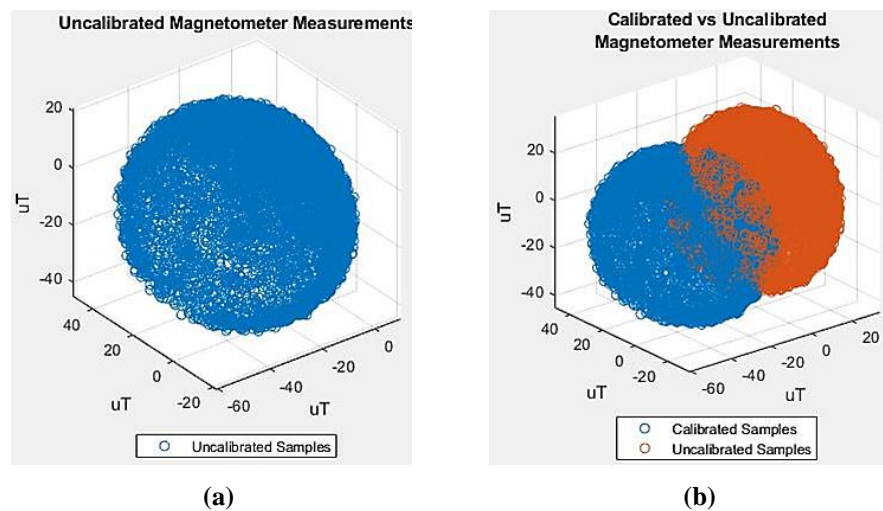


Fig. 7. Magnetometer readings. (a) Uncalibrated data; (b) Comparison between uncalibrated and calibrated data

The correction matrix obtained for Soft-iron shown in Eq. (4) is a non-identical matrix and there are corrective values of Hard-iron matrix shown in Eq. (5) which means that there is an interference from both Soft-iron and Hard-iron errors. Figure 7(b) shows a comparison between uncalibrated and calibrated data where the calibrated data is placed in a perfect sphere centred at the origin.

Generally, Hard-iron and Soft-iron errors produced by the sensor can affect the accuracy of yaw angle reading. These types of errors can be calibrated in MATLAB software that uses a variety of solvers to produce correction parameters as inputs for the measurement of new magnetometer data. This parameter can correct the uncalibrated data which can transform an offset ellipsoid to lie on the ideal sphere, centered on the origin. Experimental results of magnetometer calibration indicate that the accuracy of data collection in terms of yaw angle has been greatly enhanced.

The MPFI sensor was tested twice to obtain velocity and displacement as shown in Figs. 8-11. Figures 12 (a) and (b) show the final position of the MPFI sensor

after slope failure from the first and second experiment respectively. The negative values of the data shown in Figs 8-11 are due to the orientation of the MPU-9250 sensor. In the first experiment, the data shown in Figs. 8 and 9 are linear when the load is applied, and the movement on the x-axis begins to show significant changes after 6.4 seconds with a velocity of 1.42m/s. For the second experiment, the pattern for velocity and displacement data shown in Figs. 10 and 11 are the same as the first experiment but the slope movement on the x-axis shows significant changes after 6.8 seconds with a velocity of 1.44 m/s.

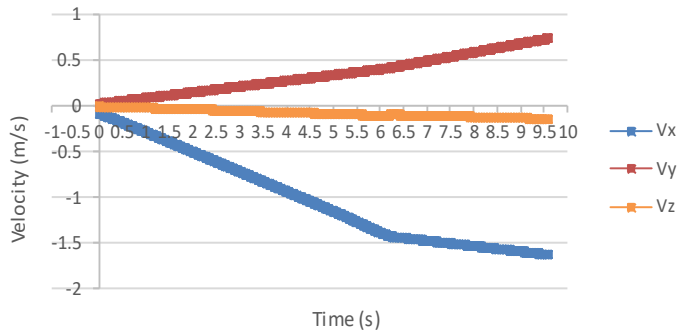


Fig. 8. The velocity of slope movement from first experiment.

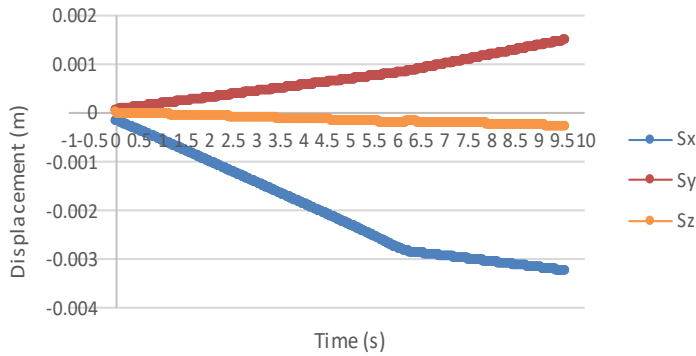


Fig. 9. The displacement of slope movement from first experiment.

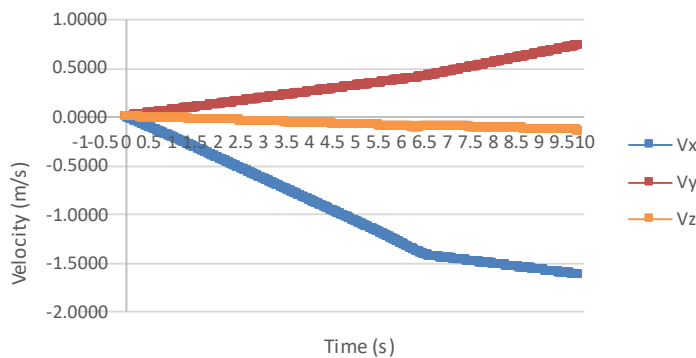


Fig. 10 The velocity of slope movement from second experiment.

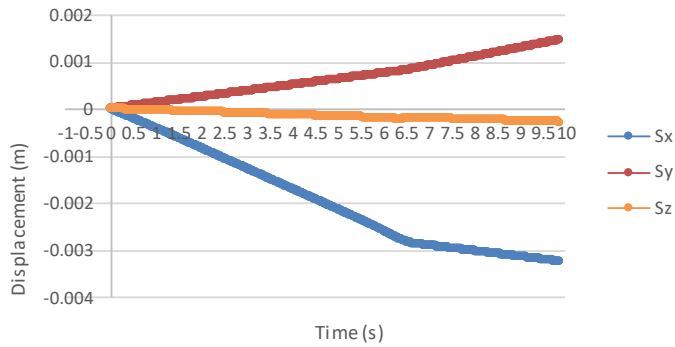


Fig. 11. The displacement of slope movement from second experiment.

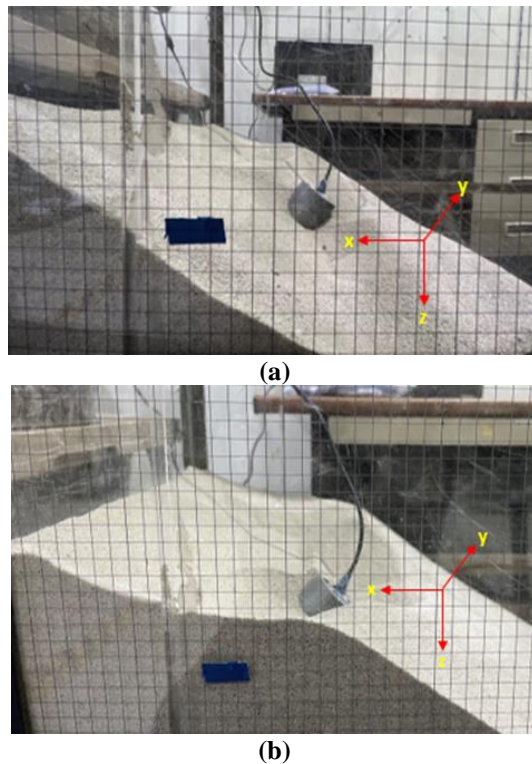


Fig. 12. Position of MPFI sensor after the slope failure.
(a) First experiment; (b) Second experiment.

The sensor fusion of gyroscope, accelerometer, and magnetometer may reduce and overcome the error occurred. This shows that the concept of data fusion should be applied in slope monitoring system as high precision of data measurement can be obtained. Most importantly, things that need to be given attention when using inclinometer measurements is the occurrence of systematic errors as it may lead to disturbance on data measurement of slope displacements and prior to on-site sensor installation, it must be calibrated in the laboratory as more accurate real-time data collection can be obtained.

4. Conclusions

The average velocity from the first experiments for the x, y and z axes are 1.02m/s, 0.35m/s and 0.08m/s, while from second experiment are 0.98m/s, 0.33m/s and 0.07m/s respectively. The concept of MPFI development has been described in general. In addition, data calibration has been adopted in this study to obtain high accuracy data and make the performance of the slope monitoring system more reliable.

The newly developed inclinometer sensor can provide data of slope movement in 3-dimensions in terms of velocity and displacement. As a result, it can provide more accurate and reliable data to the authorities in the future to make risk slope assessments. Nevertheless, the application of the proposed inclinometer sensor for real-time slope movement detection will continue to be developed, where changes in the threshold values of slope movement as well as the possibility of slope failure can be detected.

Generally, slope failure is a sudden event that can adversely affect infrastructure and human life. A good technique with the application of latest technology is essential for developing a real-time slope monitoring system. It is important to use appropriate techniques based on the geological environment and available advantages to provide good data information about slope movement rates and types of slope failures as well as to avoid failures in data processing.

The accuracy of the application of inclinometer sensor in slope monitoring depends on many factors. Other than geological conditions, the design of sensor and the quality of the inclinometer play an important role to get a more accurate reading of data. Moreover, a proper planning on the external structure design such as the inclinometer casing, probe and cable is crucial for a better performance of data collection.

Acknowledgments

The authors wish to express gratitude to the National Defence University of Malaysia for funding and supporting the completion of this project under the grant with the project code PS0017-UPNM/2021/GPPP/TK/9.

Nomenclatures

C_S	Soft-iron correction matrix
C_H	Hard-iron correction matrix

Greek Symbols

φ	Angle of pitch, deg
ϑ	Angle of yaw, deg
ρ	Angle of roll, deg.
ω	Angular velocity, deg.

Abbreviations

AE	Acoustic Emission
DMP	Digital Motion Processor
FBG	Fiber Bragg Grating
IMU	Initial Measurement Unit

MEMS	Micro-Electromechanical System
MPFI	Multi-Point Fixed Inclinometer
TDR	Time Domain Reflectometry

References

1. Jelani, J.; Hah, M.S.A.; Mohd Daud, M.N.; Ahmad, N.; Othman, M.; and Wan Mohamed Sabri, W.M.S. (2021). Stability analysis of a man-made slope: a case study on the UPNM campus, Sg Besi, Kuala Lumpur. *Sustainable Development of Water and Environment, Proceedings of the ICSDWE2021*, 39-46.
2. Jelani, J.; Baharudin, S.; Othmana, M.; Mohd Daud, M.N.; Ahmad Ishak, A.S.; and Yahya, M.A. (2021). Preliminary investigation of the effect of surcharge load and distance on non-homogenous man-made slope. *Jurnal Kejuruteraan SI*, 4(1), 101-107.
3. Vega, J.A.; Marín, N.J.; and Hidalgo, C.A. (2019). Statistical approaches for the assessment of landslide-related economic losses. *IOP Conference Series: Materials Science and Engineering*, 471(10), 1-8.
4. Wu, H.; Guo, Y.; Xiong, L.; Liu, W.; Li, G.; and Zhou, X. (2019). Optical fiber-based sensing, measuring, and implementation methods for slope deformation monitoring: a review. *Journal of IEEE Sensors*, 19(8), 2786-2800.
5. Abdul Rahman, H. and Mapjabil, J. (2017). Landslide disaster in Malaysia: an overview. *Journal of Health and the Environmental*, 8(1), 58-71.
6. Chae, B.G.; Park, H.J.; Catani, F.; Simoni, A.; and Berti, M. (2017). Landslide prediction, monitoring and early warning: a concise review of state-of-the-art. *Journal of Geosciences*, 21(6), 1033-1070.
7. Noor, M.M.; Muda, M.A.; and Rahman, A.A. (2019). Rainfall induced slope failure detection using infiltration type slope stability method applying non-linear failure envelope. *IOP Conference Series: Materials Science and Engineering*, 513(1), 1-9.
8. Yang, P.; Wang, N.; Jiang, Z.; Yang, Y.; and Yan, H. (2019). Overview of slope monitoring technology. *IOP Conference Series: Materials Science and Engineering*, 472(1), 1-5.
9. Giri, P. (2018). *Landslide monitoring and warning using wireless sensor network system*. Ph.D. Thesis. Department of Civil & Architectural Engineering, University of Wyoming, United States.
10. Codeglia, D.; Dixon, N.; Fowmes, G.J.; and Marcato, G. (2017). Analysis of acoustic emission patterns for monitoring of rock slope deformation mechanisms. *Journal of Engineering Geology*, 219, 21-31.
11. Yadav, D.K.; Karthik, G.; Jayanthu, S.; and Das, S.K. (2019). Design of real-time slope monitoring system using time-domain reflectometry with wireless sensor network. *Journal of IEEE Sensors*, 3(2), 1-4.
12. Zheng, Y.; Huang, D.; and Shi, L. (2018). A new deflection solution and application of a fiber bragg grating-based inclinometer for monitoring internal displacements in slopes. *Journal of Measurement Science and Technology*, 29(5), 1-11.

13. Bunawan, A.R. (2020). *Development of slope monitoring device using accelerometer*. Ph.D. Thesis. School of Civil Engineering, Universiti Teknologi Malaysia, Malaysia.
14. Łuczak, S. (2014). Guidelines for tilt measurements realized by MEMS accelerometers. *International Journal of Precision Engineering and Manufacturing*, 15(3), 489-496.
15. Łuczak, S.; Grepl, R.; and Bodnicki, M. (2017). Selection of MEMS accelerometers for tilt measurements. *Journal of Sensors*, 2017, 1-13.
16. Hoang, M.L. and Pietrosanto, A. (2020). An effective method on vibration immunity for inclinometer based on MEMS accelerometer. *International Semiconductor Conference (CAS)*, 105-108.
17. Pang, Y.; Song, N.; Yang, Y.; Liang, J.; Zhang, H.; Tian, L.; Liu, Z.; and Ma, F. (2021). Low-cost IMU error inter-correction method for verticality measurement. *Journal of IEEE Transactions on Instrumentation and Measurement*, 70, 1-14.
18. Wu, H.; Pei, X.; Li, J.; Gao, H.; and Bai, Y. (2020). An improved magnetometer calibration and compensation method based on Levenberg-Marquardt algorithm for multi-rotor unmanned aerial vehicle. *Journal of Measurement and Control*, 53(3-4), 276-286.